

Formation of quasiperiodic patterns within a simple two-dimensional model system

A. Quandt and M. P. Teter

Laboratory of Atomic and Solid State Physics, Cornell University, Ithaca, New York 14853-2501

(Received 6 August 1998)

We present a simple two-dimensional model system which tends to organize itself in the form of a quasiperiodic state. The system is composed of one sort of particles only, with mutual interactions that strongly deviate from the standard Lennard-Jones-type of potentials at intermediate distances. The dynamics of this system are simulated by using standard molecular dynamics methods for classical systems.

[S0163-1829(99)01913-X]

I. INTRODUCTION

Due to the discovery of quasicrystals¹⁻³ it became very clear that the (modulated) crystalline and the amorphous state are not the only possible ways for particles to aggregate into a solid form. However, the way in which the aggregation of the quasicrystalline state takes place is still a puzzle.

One empirical finding which might give a hint about the mechanisms behind the formation of quasicrystals is the fact that, so far, all known quasicrystals are at least binary alloy systems.⁴ The usual way to explain their formation is based on *Hume-Rothery* types of stabilization mechanisms (for a brief discussion see Refs. 5 or 6).

The most serious drawback in trying to establish this theory lies in the fact that up to date, all of these considerations are basically static: Usually one has to deal with very large many-particle systems that can only be treated numerically as long as the ionic cores of the constituent atoms are kept frozen. Consequently the only dynamical part of these considerations is the structure determination of the crystallographers, and any major revision of existing structure models carries with it the danger that the refined stable structures might suddenly turn out to break the “well established” Hume-Rothery rules.

There has also been a long tradition of severe criticism of the Hume-Rothery type of stabilization mechanisms, pointing out that the formation of metallic systems is primarily based on a delicate balance between pairwise central forces and volume-dependent terms, which does not necessarily have to follow the Hume-Rothery rules.⁷ This of course poses another problem: In order to examine such a hypothesis in practice, it would be necessary to determine the pairwise and volume-dependent potentials very accurately, e.g., by fitting them to precise *ab initio* data of known elemental metallic systems and simple alloys, and then run computer time expensive dynamical simulations for appropriate sample approximants. This has not been achieved to any substantial extent yet, and consequently the whole chemistry of the binding partners in quasicrystalline alloy systems remains unclear.

Another problem complicating our understanding of quasicrystal formation is the fact that the vast majority of quasicrystals may *not* be properly described on the basis of perfect quasiperiodic tilings. At least, one should take into account a serious rate of defectiveness. Alternatively, one

may assume that the formation of these phases is strongly driven by stochastic effects, i.e., by the entropic part of the free energy. This is one of the central ideas behind the random tiling model class (see⁸ and references therein). Although there has been considerable progress in understanding the growth of random tilings,^{9,10} it should not be overlooked that we hardly know anything about the interplay between the various constituents of the free energy during the formation of alloy systems, which undoubtedly would be the key to explain the formation of quasicrystals.

Being aware of the many severe problems coming with any attempt to explain the formation of quasicrystals, is quite natural to resort to simple and controllable model systems first, before going into the tedious process of more realistic simulations. Of course, with the hope that one might draw useful information from such simplified approaches, but our main results will consist of an illustration of how the basic structure elements of a quasiperiodic square-triangle-tiling¹¹ formed dynamically in a two-dimensional model system that is composed of one sort of particles only. To this end, the following section will describe the basic numerical methods used to simulate that system. Whereas the remaining sections will deal with the numerical results, as well as with a discussion of what, in our eyes, might be important in comparison to real systems.

We close the Introduction by mentioning that the results in this paper have been largely influenced by two publications,^{13,14} which demonstrated the formation of local patterns related to dodecagonal quasicrystals in three-dimensional (3D) model systems. However, we do not think that the existence of these papers makes the present study unnecessary: whether there are much simpler and more transparent model systems that show a similar behavior is a non-trivial question, and a serious test of the general findings documented in Refs. 13 or 14. Besides that, one should always keep in mind that there is an elegant and straightforward way even to connect icosahedral and dodecagonal order, based on corrugated layers made of distorted and undistorted tiles of a perfect 2D square-triangle tiling.¹⁵

II. OUTLINE OF METHODS

The central point in any classical molecular dynamics simulation is the way in which one chooses the classical model potential. As we are interested in the formation of

solids well below their melting points, it is quite natural to choose a binding pairwise type of potential. However, the form of the potential should leave us with enough freedom to suppress certain coordination spheres, a process which is assumed to happen quite often in real metallic systems, based on Friedel oscillations of interatomic potentials (for a brief discussion see Ref. 7).

For the two-dimensional simulations to be discussed, we consequently chose the following type of potentials $V(r_{ij})$:

$$V(r_{ij}) = \left[s_0 \left(\frac{4}{r_{ij}^{12}} - \frac{4}{r_{ij}^6} \right) + \sum_m S_m G_m \right] \times F_s, \quad (1)$$

$$G_m = \exp \left[- \left(\frac{r_{ij} - c_m}{w_m} \right)^2 \right], \quad (2)$$

$$F_s = \left[1 - \frac{r_{ij}^4}{r_c^4} \right]^2, \quad (3)$$

where $r_{ij} = |\vec{r}_i - \vec{r}_j|$ for particles located at \vec{r}_i , respectively, \vec{r}_j , and r_c being a suitably chosen cutoff radius (see also Table I).

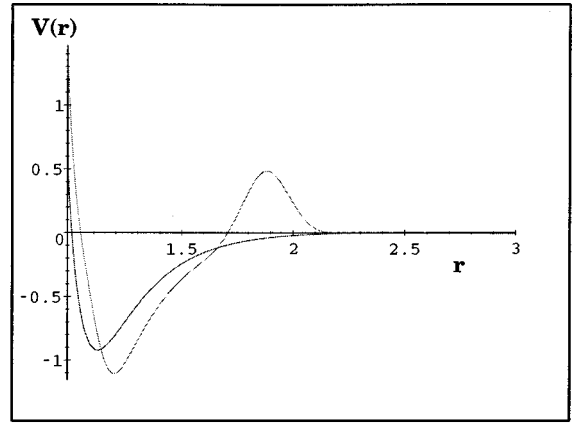
We notice that the basic potential is of Lennard-Jones (LJ) type, and indeed all basic units are related to the standard unit systems in use for such systems (e.g., see Ref. 12). But we also decided to add one or more Gaussians G_m to the LJ potential whenever necessary. The role of these Gaussians is diverse: They can be used to shift minima, to narrow the regime of favorable bond length, or to suppress certain coordination spheres of stable geometries usually reached by the unperturbed model system. When carrying out actual simulations, we found that the rational approximation to the Gaussians

$$\exp(-r^2) \approx \frac{1}{(1 + r^2/12 + r^4/288)^{12}} \quad (4)$$

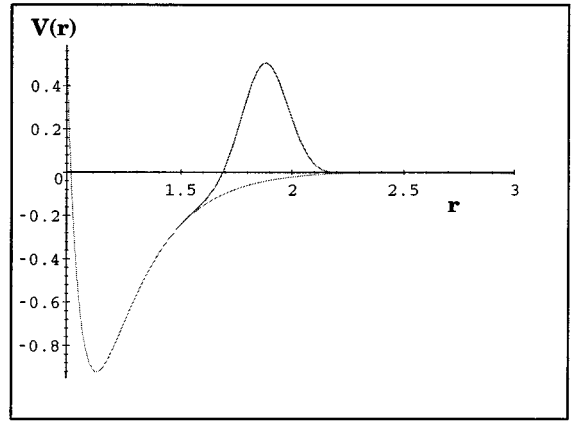
worked very well, especially in speeding up the simulations enormously.

Finally we would like to modify the potentials such that we get rid of the long-range tail of the potential by multiplying it with a cutoff factor F_s , which adjusts the potential to go to zero at the cutoff radius r_c . Beyond that radius, the potential will be set equal to zero. This of course is not the case in Fig. 1. There we extended the range beyond the cutoff radius, as an easy check that the potential has properly gone to zero at r_c , and then bounced off due to the symmetric nature of the smoothing factor around r_c .

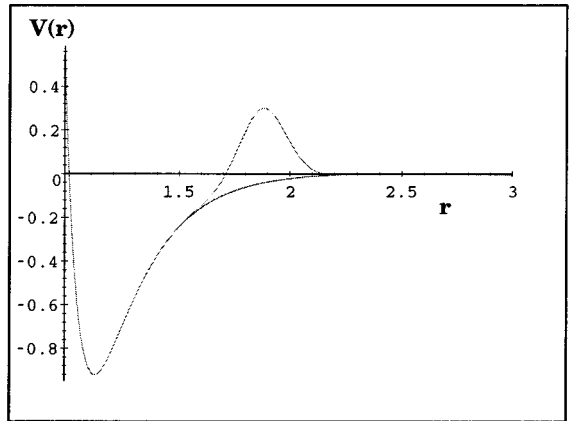
The molecular dynamics simulations themselves have been kept as simple as possible. We took the major routines from Ref. 12, which should make the present results transparent and easily reproducible. Major modifications were only necessary when implementing the general type of potentials described above, and in connection with our need to obtain a formatted input and output from the program. A formatted output was very helpful when checking the results, restarting the program from previous simulations, and in order to produce an output that could be read into MAPLE V. We used the latter to produce the graphics (of course with the exception of the diffraction spectra shown below), but also to



(a)



(b)



(c)

FIG. 1. Pictures of the potentials tabulated in Table I. (a) Lennard-Jones potential (type 1, without bump) and modified potential with two Gaussians added (type 2). (b) Modified potential with one Gaussian added (type 3) and the Lennard-Jones potential (type 1) as a reference. (c) Modified potential (type 4), with a moderately high Gaussian bump added to it. Note that the values of the potential $V(r)$ and of the interatomic distances r are in standard units of Lennard-Jones type of potentials.

check the calculation of derivatives based on Eqs. (1)–(3), which is a very tedious exercise.

Among the features going into the program, we used a predictor-corrector mover,¹² imposed constant temperature by velocity rescaling,¹² and sped up the calculation of forces

TABLE I. List of potential parameters. The parameters, which characterize the basic Lennard-Jones potential and the Gaussians added to it, are explained in connection with Eqs. (1)–(3). All parameters must be thought relative to the basic units of Lennard-Jones type of potentials. Pictures of these potentials are shown in Fig. 1.

Type	s_0	s_1	c_1	w_1	s_2	c_2	w_2	r_c
1	1.0							2.5
2	1.5	1.2	1.9	0.15	1.0	1.05	0.1	2.5
3	1.0	1.2	1.9	0.15				2.5
4	1.0	0.75	1.9	0.15				2.5

and potentials using a linked cell technique as described in Ref. 12. The volume was kept fixed throughout all simulations, and we imposed periodic boundary conditions onto the system. The resulting program was then checked against the results given in the literature, e.g., concerning results for soft-sphere potentials described in Ref. 12 itself, but also by carrying out a rough travel through the phase diagrams for LJ type of potentials, which are, e.g., described in Ref. 16.

The diffraction spectra were evaluated using a program of D. Joseph (Cornell/MPI Dresden) designed for two-dimensional systems. The basis for calculating the peak intensities $I(\vec{k}_j)$ given a set of mesh points $[\vec{k}_j]$ in k space is very simple:

$$I(\vec{k}_j) \equiv N^{-1} \left| \sum_n \exp(i\vec{k}_j \cdot \vec{r}_n) \right|^2, \quad (5)$$

where N is the number of atoms in the unit cell, and the set of all r_n comprises the respective locations of the atoms within the unit cell.

Let us close this section by recalling the features that a potential chosen according to Eqs. (1)–(3) will lack in comparison to realistic metallic systems: First one physical dimension, second all kinds of volume-dependent interactions, which of course is a minor flaw as we kept the volume of the unit cell constant, and third all kinds of angular-dependent interactions. Despite these problems, the model potential chosen is not very different in nature from other types of potentials that have been used for qualitative studies in a metallic system.¹⁷ We explicitly recommend to browse through the latter monograph,¹⁷ not only for the sake of comparison with the model potentials chosen, but also for making up one’s mind about the astonishing diversity of “qualitative” model potentials chosen for transition metals, as well as for Al. This fact illustrates rather nicely the abovementioned technical difficulties in fitting appropriate model potentials for realistic intermetallic systems.

III. NUMERICAL RESULTS

The simulations described in this paper were all carried out at a fixed temperature $T=0.15$ and a fixed density of $\rho=0.82$, starting from a homogeneous cubic arrangement of atoms. The optimal time steps for the mover were found to be $\Delta t=0.001$.

The way in which we determined these values of T and ρ was more or less by *trial and error*. One could call it “vir-

TABLE II. Data characterizing the simulation runs. “Steps” denotes the number of time steps, and “sample” denotes the size of the system. The label of the potentials refers to Table I. The (r) , appearing after the number of time steps, is thought to indicate a restart from a previous simulation. It should be noted that *all* simulations were carried out at a temperature $T=0.15$ and a density $\rho=0.82$.

No.	steps	size	potential
1	100 000	900	1
2	100 000	900	2
3	100 000	900	3
4	100 000	900	4
5	200 000 (r)	900	4
6	100 000 (r)	900	4
7	200 000	1600	4
8	300 000 (r)	1600	4

tual metallurgy,” as at the beginning we were just blindly shifting through the phase diagrams trying to produce as many crude samples as possible and looking for a certain trend which might lead us to quasicrystalline patterns. Thus the material presented in this paper is more or less the very best of all those crude trials. This situation is quite comparable to the few good quasicrystals compared to the many imperfect alloy samples disappearing in the laboratory waste baskets over the years.

We usually started our series of simulations within a high- or low-density domain, seeking to stabilize the (lowest possible) pressure on the system without creating too much structural defects. Let us illustrate this in the following, starting from Table II.

As one can see, the first three simulations were carried out on the same set of 900 atoms, but using quite different types of potentials. The first simulation was based on a smoothed LJ potential (see Fig. 1). The result of the simulation run is shown in Fig. 2. Obviously, we did not choose the optimal density to fill the simulation box. There are wide areas of holes and structural defects within the sample. Nevertheless such samples are very useful when examining the time evolution of structural defects, e.g., as described in Ref. 17. We also see that the smoothed LJ sample has a tendency to crystallize in the form of a hexagonal lattice. The reason why we did not show a diffraction pattern for this sample is pretty clear: no crystallographer would ever use such a bad sample; or he would rather cut it into pieces, and carry out some sort of powder diffraction.

For the second sample, we added two Gaussians to the LJ potential. Their effect was to shift and narrow the minimum of the potential, but we also used them to suppress a certain range of bonding distances (see Fig. 1). Let us have a look at the results (Fig. 2). Obviously, the shift of the minimum r_{\min} in the potential forces the particles to longer mutual bonding distances—as a consequence, the simulation box is nearly homogeneously filled.

We also see that the effect of the outermost Gaussian remains to sharpen the minimum, only. In order to suppress the second coordination sphere of the resulting triangular lattice effectively, the Gaussian should have been placed closely to a distance of $1.732r_{\min}$, which means roughly at

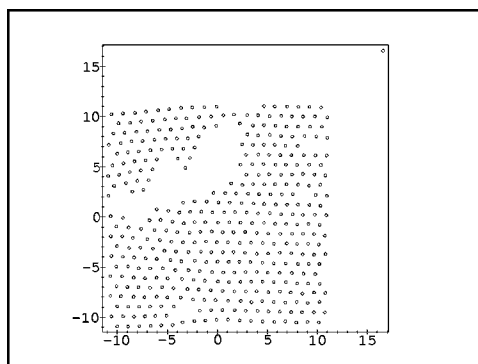
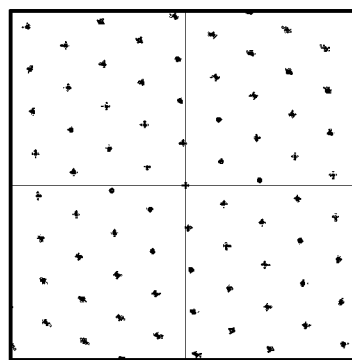
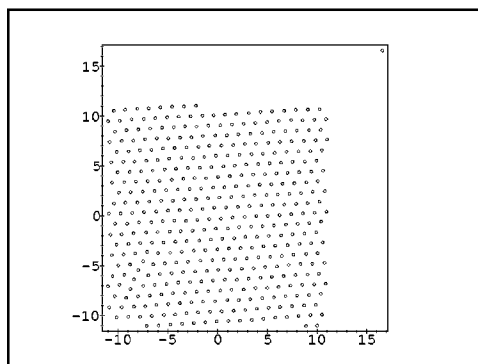
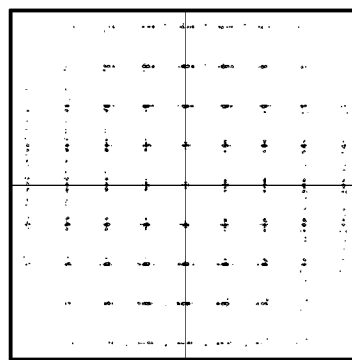
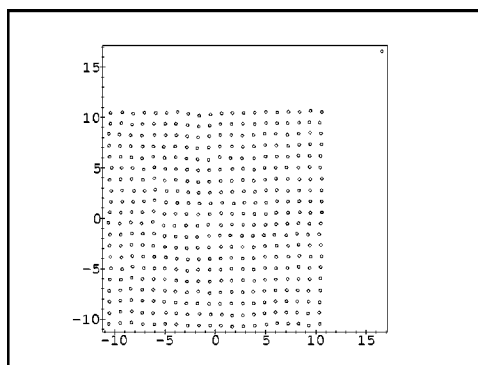
**Sample 1****Sample 2****Sample 3**

FIG. 2. Structure and diffraction spectra of the generated samples (I). The frame to the left contains a clip from within the center of the sample, comprising about 400 atoms. The lonely “atom” in the corner has been added to mark one of the vertices of the simulation box, in order to illustrate the location of the clip within the sample. The box dimensions are given in basic units of length scale for Lennard-Jones potentials. The frame to the right contains the diffraction patterns for a complete atomic arrangement within the simulation box.

$r=2.1$, as simple geometrical calculus shows. Such numbers should, of course, be taken with a grain of salt—it is very unlikely that nature will ever produce perfectly suppressing potentials with such a high precision when forming a solid state. Rather, we should expect a certain *window* of favorable bond lengths.¹⁸

The placement of the suppressing Gaussian for the third sample remained at the same place, whereas the shifting inward Gaussian was removed. The result is an impressingly high barrier, located approximately at the second coordina-

tion sphere of the triangular lattice for a LJ potential without bumps (see Fig. 1). The result of an MD simulation on such a system is documented in Fig. 2: Obviously, the starting cubic lattice mainly goes over into a slightly modulated form, which could already be seen during the simulation runs, because the overall pressure went to zero very quickly.

Such a behavior seems to make sense, as the cubic arrangement is supposed to be a configuration with optimal nearest neighbor bonding, but avoiding the unfavorable second nearest neighbor coordination shell of the triangular lat-

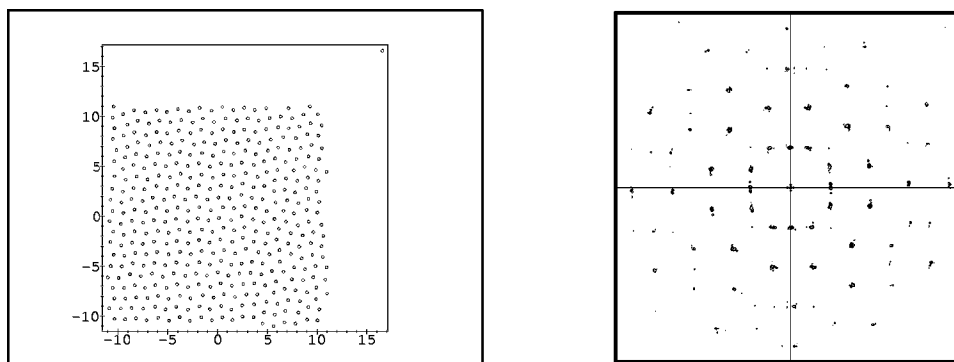
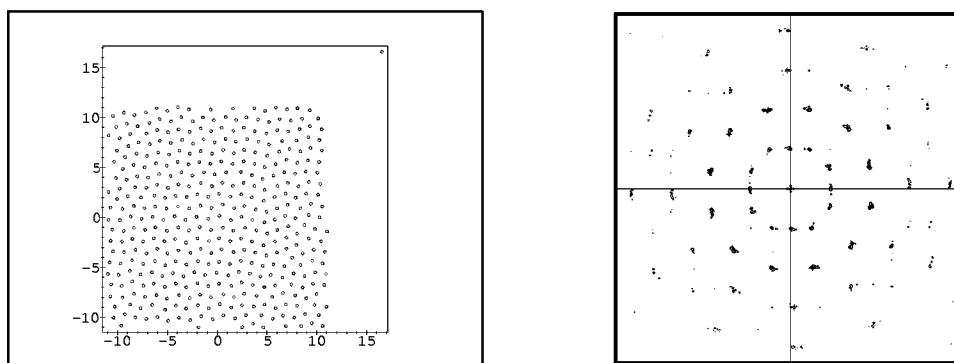
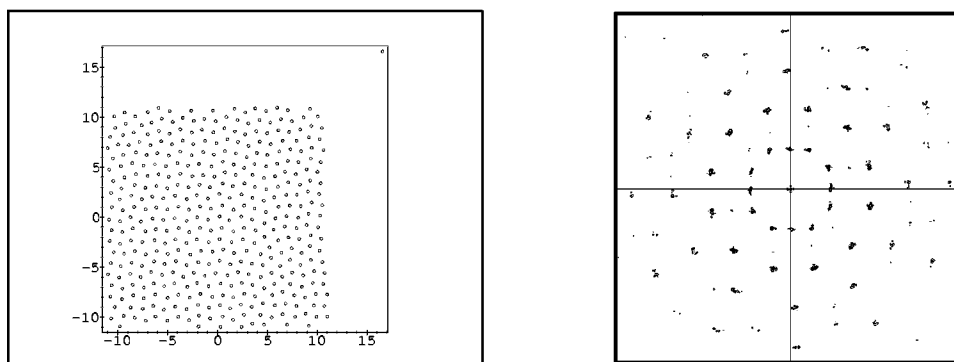
**Sample 4****Sample 5****Sample 6**

FIG. 3. Structure and diffraction spectra of the generated samples (II). For explanations see Fig. 2.

tice. Of course the packing density of these systems is considerably lowered by such an arrangement, and we found that the binding energy per particle used to drop considerably.

The next step in changing our potential is pretty clear: lower the suppressing Gaussian, such that there will be a broader range of favorable coordination shells (see Fig. 1). The result is pretty amazing—once again the system contracts, but this time, squares *and* triangles are formed, and, even better, the arrangement of the particles leads to 12-fold symmetric diffraction patterns, as to be expected for an *approximant* to the square-triangle tiling (see Fig. 3). We also found that the binding energy per atom slightly raised during

the formation of this pattern, certainly due to an improved average local coordination of the atoms.

Now the question arises whether the formation of these patterns might just be an artifact, which will go away after a longer simulation period of time. Consequently we extended the simulation times from 100 000 simulation steps up to 400 000 simulation steps (see Table II). It is very obvious (Fig. 3) that we found an improvement in the quality of the samples, rather than a deterioration (Fig. 3).

An usual problem is created by finite size effects on the results. Here, we can only show that when raising the number of particles moderately from 900 to 1600, and even after

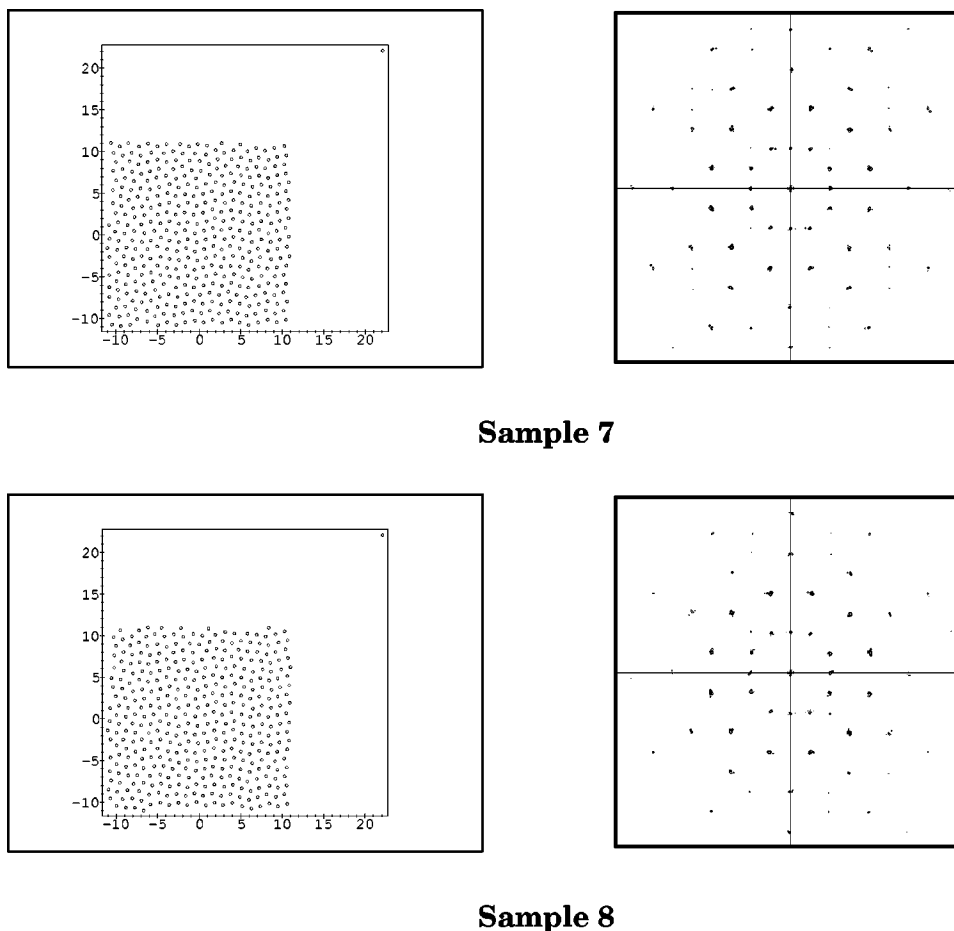


FIG. 4. Structure and diffraction spectra of the generated samples (III). For explanations see Fig. 2.

500 000 time steps, we could not observe noticeable changes in the behavior of the system (see Fig. 4), other than the fact that the evolution of the square-triangle patterns proceeds somewhat slower than before. Nevertheless, we cannot exclude such finite size effects, and therefore our study might shed some light on the formation of local square-triangle patterns, but not necessarily on the formation of the quasicrystal bulk itself similar to, e.g., the remarkable results documented in Refs. 9, 10.

Let us finally say a few words about the detailed structure of the diffraction patterns. It might be important to note that we have suppressed the diffuse background existing in any of the 12-fold symmetric patterns depicted here, just for reasons of beauty. The existence of such a background in principle points towards a random tiling type of model,¹⁹ which in turn would suggest a random tiling idealization of our results. However, we would feel unreliable when recommending to see the mere existence of this background as a hint for random effects influencing our results, for the following reason: A more precise look at the inner ring reveals that these peaks are not located at the proper positions of a perfect 12-fold symmetric diffraction pattern, but more or less close to them. Consequently, the patterns we see are, strictly speaking, only approximants to a proper square-triangle tiling (see above).

Rather we would like to argue on the basis of the obvious improvement in the intensity of the main diffraction peaks indicated above, which became more pronounced the longer

we ran the simulations: there we could hardly observe any change in the binding energies other than small fluctuations, while the sample obviously improved its aggregation in the form of a square-triangle tiling. We think that this is the strongest indication for entropic effects that we are able to give so far. A more careful examination of diffraction patterns and their interpretation for the present system, as well as for a series of improved model systems, must be the topics of future publications.

IV. DISCUSSION

We carried out a series of simulations on two-dimensional model systems using a family of pairwise model potentials. We showed that, given a certain (empirically determined) optimal temperature and density, the system evolves into a structure that forms local square-triangle patterns. The key for this process seems to be the “partial suppression” of the second coordination sphere for a triangular lattice in 2D, the usual ground state obtained with “unsuppressed” potentials.

It is possible that similar mechanisms may also play a certain role in realistic quasicrystalline systems, as pointed out in Ref. 18. Nevertheless, understanding the real nature of the metallic phase certainly requires a much higher level of accuracy than the one chosen for this study. Among the most important features of realistic metallic systems will be a certain type of angular dependence and, even more important, the abovementioned delicate interplay between volume-

dependent interactions and pairwise interactions. This leaves such systems with a nontrivial density dependence, something we completely neglected throughout this study.

There is of course another point that ought to be mentioned here, and which makes the present study especially interesting: *boron*. In fact, any (naive or elaborate) construction of structure models for icosahedral quasicrystals somehow starts from icosahedral clusters, seeking ways of sticking them together to form the basic rhombohedral unit cells of the tiling superstructure.⁴

The surprising fact is that boron does all that—it aggregates into solid structures based on icosahedral clusters, and especially in the form of a unit cell which is only a slightly distorted variant of a prolate rhombohedral unit cell necessary to form a quasicrystal, and even the corresponding oblate unit cell may theoretically be composed as a network of stable icosahedral and tubular clusters.²⁰ All of this quite naturally leads to the hypothesis that the quasicrystalline state could be one of the possible modifications of the *pure element* boron.

However, nobody has been able to find this one-elemental boron quasicrystal so far, and the reason for that is, at least for the authors of this paper, as amazing as the formation of quasicrystalline alloy systems themselves. Maybe simulations such as the present one in 3D, as already carried out in Refs. 13 and 14, but of course properly taking into account the delicate nature of boron bonding, might bring with them some progress in understanding this interesting problem.

ACKNOWLEDGMENTS

The authors would like to thank Veit Elser (Cornell) and Dieter Joseph (Cornell/MPI Dresden) for many helpful discussions. We also thank Dieter Joseph for providing and implementing a program to evaluate diffraction spectra for two-dimensional structures. This work was supported by NSF Grant No. DMR-9520315 and by the Deutsche Forschungsgemeinschaft under Project No. Qu 119/1.

¹D. Shechtman, I. Blech, D. Gratias, and J. W. Cahn, *Phys. Rev. Lett.* **53**, 1951 (1984).

²T. Ishimasa, H.-U. Nissen, and Y. Fukano, *Phys. Rev. Lett.* **55**, 511 (1985).

³L. Bendersky, *Phys. Rev. Lett.* **55**, 1461 (1985).

⁴C. Janot, *Quasicrystals, A Primer (Second Edition)* (Clarendon, Oxford, 1994).

⁵D. Pettifor, *Bonding and Structure of Molecules and Solids* (Clarendon, Oxford, 1995).

⁶D. Mayou, in *Lectures on Quasicrystals*, edited by F. Hippert and D. Gratias (Les Editions de Physique, Les Ulis, 1994).

⁷V. Heine and D. Weaire, in *Solid State Physics*, edited by H. Ehrenreich, F. Seitz, and D. Turnbull (Academic, New York, 1970), Vol. 42.

⁸C. Richard, M. Höffe, J. Hermisson, and M. Baake, *J. Phys. A* **31**, 6385 (1998).

⁹D. Joseph and V. Elser, *Phys. Rev. Lett.* **79**, 1066 (1997).

¹⁰D. Joseph, *Phys. Rev. B* **58**, 8347 (1998).

¹¹M. Baake, R. Klitzing, and M. Schlottmann, *Physica A* **191**, 554 (1992).

¹²D. C. Papaport, *The Art of Molecular Dynamics Simulation* (Cambridge University Press, Cambridge, 1997).

¹³M. Dzugutov, *Phys. Rev. A* **46**, R2984 (1992).

¹⁴M. Dzugutov, *Phys. Rev. Lett.* **70**, 2924 (1993).

¹⁵R. Wittmann, *Z. Kristallogr.* **213**, 79 (1998).

¹⁶R. Balescu, *Equilibrium and Nonequilibrium Statistical Mechanics* (Wiley, New York, 1975).

¹⁷*Interatomic Potentials and Crystalline Defects*, edited by J. K. Lee (The Metallurgical Society of AIME, Warrendale, PA, 1981).

¹⁸N. W. Ashcroft, *Nuovo Cimento D* **12**, 597 (1990).

¹⁹A. Hof, *Commun. Math. Phys.* **169**, 25 (1995).

²⁰I. Boustani, A. Quandt, and P. Kramer, *Europhys. Lett.* **36**, 583 (1996).